Inner retinal metabolic rate of oxygen by oxygen tension and blood flow imaging in rat

Justin Wanek, Pang-yu Teng, John Albers, Norman P. Blair, and Mahnaz Shahidi*

Department of Ophthalmology and Visual Sciences, University of Illinois at Chicago, Chicago IL, 60612, USA
**mahnshah@uic.edu*

Abstract: The metabolic function of inner retinal cells relies on the availability of nutrients and oxygen that are supplied by the retinal circulation. Assessment of retinal tissue vitality and function requires knowledge of both the rate of oxygen delivery and consumption. The purpose of the current study is to report a novel technique for assessment of the inner retinal metabolic rate of oxygen (MO_2) by combined measurements of retinal blood flow and vascular oxygen tension (PO_2) in rat. The application of this technology has the potential to broaden knowledge of retinal oxygen dynamics and advance understanding of disease pathophysiology.

OCIS codes: (170.2655) Functional monitoring and imaging; (100.2960) Image analysis; (170.3880) Medical and biological imaging

References and links

1. S. Yoneya, T. Saito, Y. Nishiyama, T. Deguchi, M. Takasu, T. Gil, and E. Horn, "Retinal oxygen saturation levels in patients with central retinal vein occlusion," Ophthalmology **109**(8), 1521–1526 (2002).
2. W. Zhang, Y. Ito, E. Berlin, R. Roberts, and B. A. Berkowitz, "Role of hypoxia during normal retinal vessel development and in experimental retinopathy of prematurity," Invest. Ophthalmol. Vis. Sci. **44**(7), 3119–3123 (2003).
3. M. Mozaffarieh, M. C. Grieshaber, and J. Flammer, "Oxygen and blood flow: players in the pathogenesis of glaucoma," Mol. Vis. **14**, 224–233 (2008).
4. E. Stefansson, "Oxygen and diabetic eye disease," Graefes Arch. Clin. Exp. Ophthalmol. **228**(2), 120–123 (1990).
5. S. J. Cringle, D. Y. Yu, P. K. Yu, and E. N. Su, "Intraretinal oxygen consumption in the rat in vivo," Invest. Ophthalmol. Vis. Sci. **43**(6), 1922–1927 (2002).
6. V. A. Alder, J. Ben-Nun, and S. J. Cringle, "PO_2 profiles and oxygen consumption in cat retina with an occluded retinal circulation," Invest. Ophthalmol. Vis. Sci. **31**(6), 1029–1034 (1990).
7. R. D. Braun, R. A. Linsenmeier, and T. K. Goldstick, "Oxygen consumption in the inner and outer retina of the cat," Invest. Ophthalmol. Vis. Sci. **36**(3), 542–554 (1995).
8. D. Y. Yu, S. J. Cringle, P. K. Yu, and E. N. Su, "Intraretinal oxygen distribution and consumption during retinal artery occlusion and graded hyperoxic ventilation in the rat," Invest. Ophthalmol. Vis. Sci. **48**(5), 2290–2296 (2007).
9. Y. Ito and B. A. Berkowitz, "MR studies of retinal oxygenation," Vision Res. **41**(10-11), 1307–1311 (2001).
10. Y. Zhang, Q. Peng, J. W. Kiel, C. A. Rosende, and T. Q. Duong, "Magnetic resonance imaging of vascular oxygenation changes during hyperoxia and carbogen challenges in the human retina," Invest. Ophthalmol. Vis. Sci. **52**(1), 286–291 (2011).
11. S. D. Wajer, M. Taomoto, D. S. McLeod, R. L. McCally, H. Nishiwaki, M. E. Fabry, R. L. Nagel, and G. A. Lutty, "Velocity measurements of normal and sickle red blood cells in the rat retinal and choroidal vasculatures," Microvasc. Res. **60**(3), 281–293 (2000).
12. R. Tadayoni, M. Paques, A. Gaudric, and E. Vicaut, "Erythrocyte and leukocyte dynamics in the retinal capillaries of diabetic mice," Exp. Eye Res. **77**(4), 497–504 (2003).
13. W. S. Wright, J. E. Messina, and N. R. Harris, "Attenuation of diabetes-induced retinal vasoconstriction by a thromboxane receptor antagonist," Exp. Eye Res. **88**(1), 106–112 (2009).
14. L. Wang, C. Grant, B. Fortune, and G. A. Cioffi, "Retinal and choroidal vasoreactivity to altered $PaCO_2$ in rat measured with a modified microsphere technique," Exp. Eye Res. **86**(6), 908–913 (2008).
15. J. E. Grunwald, C. E. Riva, S. H. Sinclair, A. J. Brucker, and B. L. Petrig, "Laser Doppler velocimetry study of retinal circulation in diabetes mellitus," Arch. Ophthalmol. **104**(7), 991–996 (1986).

#149760 - $15.00 USD Received 24 Jun 2011; revised 29 Jul 2011; accepted 29 Jul 2011; published 9 Aug 2011

16. M. H. Cuypers, J. S. Kasanardjo, and B. C. Polak, "Retinal blood flow changes in diabetic retinopathy measured with the Heidelberg scanning laser Doppler flowmeter," Graefes Arch. Clin. Exp. Ophthalmol. **238**(12), 935–941 (2000).
17. Y. Wang, A. Lu, J. Gil-Flamer, O. Tan, J. A. Izatt, and D. Huang, "Measurement of total blood flow in the normal human retina using Doppler Fourier-domain optical coherence tomography," Br. J. Ophthalmol. **93**(5), 634–637 (2009).
18. M. Szkulmowski, I. Grulkowski, D. Szlag, A. Szkulmowska, A. Kowalczyk, and M. Wojtkowski, "Flow velocity estimation by complex ambiguity free joint spectral and time domain optical coherence tomography," Opt. Express **17**(16), 14281–14297 (2009).
19. J. Sebag, F. C. Delori, G. T. Feke, and J. J. Weiter, "Effects of optic atrophy on retinal blood flow and oxygen saturation in humans," Arch. Ophthalmol. **107**(2), 222–226 (1989).
20. T. Liu, Q. Wei, J. Wang, S. Jiao, and H. F. Zhang, "Combined photoacoustic microscopy and optical coherence tomography can measure metabolic rate of oxygen," Biomed. Opt. Express **2**(5), 1359–1365 (2011).
21. V. Jain, M. C. Langham, and F. W. Wehrli, "MRI estimation of global brain oxygen consumption rate," J. Cereb. Blood Flow Metab. **30**(9), 1598–1607 (2010).
22. R. M. Berne and M. N. Levy, *Physiology*, 2nd ed. (Mosby, St. Louis, MO, 1988).
23. M. Shahidi, J. Wanek, N. P. Blair, and M. Mori, "Three-dimensional mapping of chorioretinal vascular oxygen tension in the rat," Invest. Ophthalmol. Vis. Sci. **50**(2), 820–825 (2009).
24. M. Shahidi, A. Shakoor, N. P. Blair, M. Mori, and R. Shonat, "A method for chorioretinal oxygen tension measurement," Curr. Eye Res. **31**(4), 357–366 (2006).
25. B. A. Shapiro, W. T. Perruzi, and R. Kozelowski-Templin, in *Clinical Application of Blood Gases* (Mosby-Year Book, Inc, St. Louis, 1994), pp. 33–53.
26. J. B. West, *Pulmonary Physiology and Pathophysiology: an Integrated, Case-Based Approach*, 2nd ed. (Lippincott Williams & Wilkins, Philadelphia, PA, 2007).
27. C. F. Cartheuser, "Standard and pH-affected hemoglobin-O_2 binding curves of Sprague-Dawley rats under normal and shifted P_{50} conditions," Comp. Biochem. Physiol. Comp. Physiol. **106**(4), 775–782 (1993).
28. K. Lorentz, A. Zayas-Santiago, S. Tummala, and J. J. Kang Derwent, "Scanning laser ophthalmoscope-particle tracking method to assess blood velocity during hypoxia and hyperoxia," Adv. Exp. Med. Biol. **614**, 253–261 (2008).
29. M. Shahidi, J. Wanek, B. Gaynes, and T. Wu, "Quantitative assessment of conjunctival microvascular circulation of the human eye," Microvasc. Res. **79**(2), 109–113 (2010).
30. S. L. Meyer, in *Data Analysis for Scientists and Engineers* (Wiley, New York, 1975), pp. 39–48.
31. H. Nishiwaki, Y. Ogura, H. Kimura, J. Kiryu, K. Miyamoto, and N. Matsuda, "Visualization and quantitative analysis of leukocyte dynamics in retinal microcirculation of rats," Invest. Ophthalmol. Vis. Sci. **37**(7), 1341–1347 (1996).
32. K. Yamakawa, I. A. Bhutto, Z. Lu, Y. Watanabe, and T. Amemiya, "Retinal vascular changes in rats with inherited hypercholesterolemia—corrosion cast demonstration," Curr. Eye Res. **22**(4), 258–265 (2001).
33. D. Y. Yu, S. J. Cringle, V. A. Alder, and E. N. Su, "Intraretinal oxygen distribution in rats as a function of systemic blood pressure," Am. J. Physiol. **267**(6 Pt 2), H2498–H2507 (1994).
34. J. Brotherton, "Studies on the metabolism of the rat retina with special reference to retinitis pigmentosa. I. Anaerobic glycolysis," Exp. Eye Res. **1**(3), 234–245 (1962).
35. P. Törnquist and A. Alm, "Retinal and choroidal contribution to retinal metabolism in vivo. A study in pigs," Acta Physiol. Scand. **106**(3), 351–357 (1979).
36. L. Wang, P. Törnquist, and A. Bill, "Glucose metabolism of the inner retina in pigs in darkness and light," Acta Physiol. Scand. **160**(1), 71–74 (1997).

1. Introduction

The function of retinal tissue can be adversely affected by inadequate delivery and/or consumption of oxygen. Derangements in retinal oxygenation are thought to contribute significantly to the development of vision threatening eye diseases, including retinal vascular occlusion, diabetic retinopathy, retinopathy of prematurity, and glaucoma [1–4]. However, thus far, fundamental mechanisms that implicate oxygen in the development of retinal pathologies and impairment of retinal function are not completely understood. This is in part because measurement of oxygen consumption of the inner retina in vivo has been challenging.

The oxygen-sensitive microelectrode technique has provided direct measurements of inner retinal oxygen tension (PO_2) and oxygen consumption in the rat [5], though the assumption of one dimensional oxygen diffusion gradients from the retinal capillaries for estimation of oxygen consumption may not be valid. To circumvent the complicated three-dimensional oxygen diffusion gradients, inner retinal oxygen consumption has been estimated by occlusion of the retinal vascular supply and inspiration of 100% oxygen [6–8]. However, these measurements may not accurately reflect oxygen consumption under a normal physiological

#149760 - $15.00 USD Received 24 Jun 2011; revised 29 Jul 2011; accepted 29 Jul 2011; published 9 Aug 2011

condition. Other methods have assessed inner retinal oxygen consumption in an indirect manner. Magnetic resonance imaging has provided measurements of retinal oxygenation in response to hyperoxic inhalation challenge, though with limited depth resolution for isolating the inner retinal response [9,10]. Cell labeling and microsphere imaging methods in animals [11–14] and Doppler velocimetry techniques in humans [15–18] have measured retinal blood flow, providing only limited information about the retinal oxygen metabolic function. Combined blood flow and oxygen saturation (SO_2) measurements for estimating metabolic rate of oxygen (MO_2) have been reported in human retina [19], and more recently in human brain and mouse ear [20,21]. We report an optical imaging technique for assessing inner retinal MO_2 of rat by combined measurements of retinal blood flow and vascular PO_2.

2. Methods

2.1. Metabolic Rate of Oxygen

Inner retinal MO_2 can be calculated from retinal blood flow and vascular oxygen content measurements, according to Fick's principle [22]:

$$MO_2 = \sum_{i=1}^{n} F_{v_i} (O_{2a} - O_{2v_i}) \quad (1)$$

where F_{vi} is the blood flow in the i^{th} of n veins, O_{2a} is the oxygen (O_2) content of arterial blood, and O_{2vi} is the O_2 content of blood in the i^{th} vein. It was assumed O_{2a} is the same in all retinal arteries, and the total arterial and venous blood flows are identical. Blood flow was measured in veins because they are less affected by pulsation and have larger diameters as compared to arteries. Inner retinal MO_2 was measured both globally and locally for assessing the function of the entire retinal tissue (perfused by all retinal capillaries) and a region of retinal tissue near the optic disc (perfused by capillaries draining into several adjacent smaller veins (venules)), respectively. Global inner retinal MO_2 was derived by measuring PO_2 in all major retinal arteries and veins around the optic disc and F in all major retinal veins. Local inner retinal MO_2 was determined based on measurements of PO_2 in the major feeding artery, coupled with PO_2 and F measured in smaller draining venules.

2.2. Imaging

Vascular PO_2 was measured using our optical section phosphorescence lifetime imaging system [23,24], which combines principles of optical sectioning and phosphorescence lifetime imaging. Due to an angle between the incident laser light and imaging path, phosphorescence from structures in different retinal depths were imaged. Phosphorescence imaging was performed in 10 anesthetized Long Evans rats following intravenous injection of an oxygen-sensitive molecular probe (albumin bound Pd-porphine). Since phosphorescence emission was quenched by oxygen, its lifetime was a measure of PO_2. Phosphorescence lifetime was determined using a frequency-domain approach that involved incrementally varying the phase delay between modulated laser light and camera sensitivity. Lifetime was converted to PO_2 according to the Stern-Volmer expression: $PO_2 = 1/(\kappa_Q\ \tau) - 1/(\kappa_Q\ \tau_0)$, where τ is the phosphorescence lifetime, κ_Q is the quenching constant for the triplet-state phosphorescence probe, and τ_0 is the lifetime in a zero oxygen environment.

For global inner retinal MO_2 calculation, PO_2 was measured in major retinal arteries and veins around the optic nerve head from cross-sectional phosphorescence images, according to our previously published methodology [24]. Three repeated PO_2 measurements were averaged in each major retinal artery and vein. For local inner retinal MO_2 calculation, an enface PO_2 map of a retinal area either temporal or nasal to the optic nerve head was generated by a laser scan, as described in our previous publication [23]. Global and local MO_2 measurements were obtained in 2 separate groups of 5 rats. The O_2 content of blood was determined as the sum of oxygen bound to hemoglobin and dissolved in blood [25]. The amount of oxygen bound to

#149760 - $15.00 USD Received 24 Jun 2011; revised 29 Jul 2011; accepted 29 Jul 2011; published 9 Aug 2011

hemoglobin was calculated as the product of SO_2, the hemoglobin concentration of 14 g/dl (based on a measured mean of 14.4 ± 0.6 g/dl in 7 rats), and the oxygen carrying capacity of 1.39 mlO_2/g [26]. SO_2 was calculated from the measured PO_2 and blood pH values using the hemoglobin dissociation curve [27]. The amount of dissolved oxygen in blood was calculated as the product of oxygen solubility in blood (0.003 mlO_2/dl*mmHg) and PO_2 measurements.

Blood velocity was measured by imaging intravascular motion of fluorescent microspheres [28], within 20 minutes of phosphorescence imaging. The method involved intravenous injection of 2 micron fluorescent spheres, while the retina was imaged using a prototype slitlamp biomicroscope. The slitlamp was equipped with a 488 nm diode laser for illumination and a 560 ± 60 nm emission filter placed in front of a charge-coupled device camera, which had high sensitivity and image acquisition rate. The movement of microspheres in the retinal vasculature was captured by a sequence of images acquired at a frame rate of 60 or 108 Hz. A higher acquisition rate was preferred for measuring higher blood velocity in the major retinal veins. Images were analyzed to measure the displacement of microspheres over time and derive blood velocity measurements. Blood velocity was determined based on measured velocities of 4 to 47 microspheres in major retinal veins and 1 to 10 microspheres in retinal venules. The number of microspheres visualized depended on the duration of image acquisition, and the concentration and volume of the injected microspheres, which were progressively optimized as the technique was developed. Blood vessel diameter was measured from red free retinal images for veins and from fluorescein angiograms for venules, which provided better contrast for visualization of the smaller blood vessels. Diameters were measured based on the full width at half maximum of an intensity profile of a line perpendicular to the centerline of the blood vessel, similar to our previous publication [29]. Blood vessel diameter was derived by averaging 3 to 38 measurements in major retinal veins and 2 to 19 measurements in retinal venules. The number of measurements was dependent on the length of the centerline that could be identified from the image of the blood vessel. F was calculated by the following equation: F = blood velocity*π*diameter^2/4.

3. Results

3.1. Global Inner Retina MO_2

Figure 1a shows an example of a retinal image acquired in one rat, with major retinal arteries and veins labeled. An example of a retinal vein with edges outlined based on multiple diameter measurements is shown. The locations of a single microsphere traversing a major

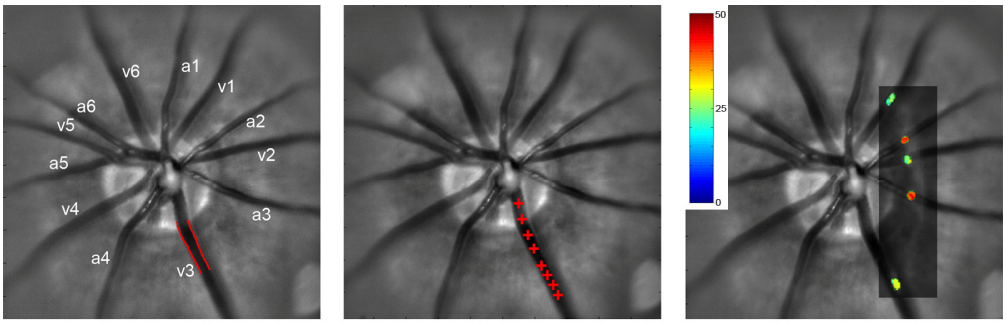

Fig. 1. (a) Retinal image with major arteries and veins labeled (a and v); the outlined edges of a vein (v3) were identified by multiple diameter measurements; (b) Red crosses overlaid on the retinal image indicate the positions of a microsphere traversing a vein (v3), visualized over 8 consecutive images; (c) A cross-sectional vascular PO_2 map (rectangle) overlaid on the retinal image, depicting values in veins (v1, v2, v3) and arteries (a2, a3). Color bar displays PO_2 in mmHg.

#149760 - $15.00 USD Received 24 Jun 2011; revised 29 Jul 2011; accepted 29 Jul 2011; published 9 Aug 2011

retinal vein as visualized over 8 consecutive images is depicted in Fig. 1b. A cross-sectional vascular PO_2 map overlaid on the retinal image is shown in Fig. 1c. Major retinal arteries and veins were differentiated based on the direction of F and level of PO_2.

Measured blood vessel diameter, velocity, PO_2, and calculated F and O_2 content of blood in the major retinal veins of a rat (shown in Fig. 1) are listed in Table 1. Since retinal arterial PO_2 is assumed to be constant, an average PO_2 over all major retinal arteries was calculated. Following Eq. (1), global inner retina MO_2 was calculated to be 639 nlO_2/min. Global inner retinal MO_2 in rats was on average 499 ± 117 nlO_2/min (N = 5).

For global MO_2 measurements, the standard deviations (SD) of repeated vessel diameter, blood velocity, and PO_2 measurements in the major retinal blood vessels were on average 3 microns, 6 mm/s, and 2 mmHg (N = 5), respectively. Using principles of propagation of error [30], the SD of MO_2 was estimated to be approximately 46 nlO_2/min, indicating changes of 90 nlO_2/min can be detected with 95% confidence.

Table 1. Vessel diameter, blood velocity, and blood flow in major retinal veins; PO_2 and O_2 content in major retinal veins and averaged over major retinal arteries (mean ± SD) in one rat

Blood Vessel	Diameter (μm)	Velocity (mm/s)	Flow (μl/min)	PO_2 (mmHg)	O_2 Content (mlO_2/dl)
Arteries				42 ± 2	11.1 ± 0.6
Vein 1	42	13	1.1	25	5.0
Vein 2	49	11	1.3	26	5.4
Vein 3	67	13	2.7	27	5.6
Vein 4	61	13	2.4	26	5.4
Vein 5	40	9	0.7	26	5.4
Vein 6	60	14	2.4	22	4.0

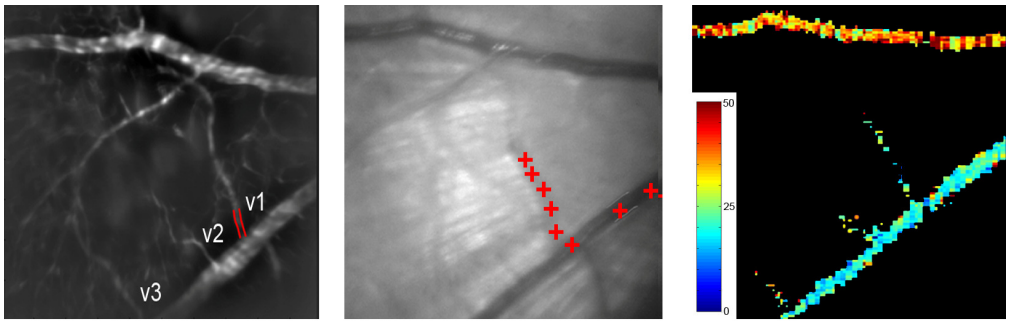

Fig. 2. (a) Fluorescein angiogram with draining retinal venules labeled; edges of a venule (v1) are outlined; (b) Red crosses overlaid on the retinal image indicate the positions of a microsphere traversing a venule (v1) and major vein, visualized over 8 consecutive images; (c) An enface PO_2 map depicting values in a segmented major retinal artery, vein, and venules. Color bar displays PO_2 in mmHg.

3.2. Local Inner Retina MO_2

Figure 2a shows an example of a fluorescein angiogram acquired in one rat, with selected retinal blood vessels numbered and labeled. The positions of a microsphere traversing a venule and a major retinal vein, overlaid on a retinal image, are shown in Fig. 2b. In Fig. 2c, an enface PO_2 map of a segmented major retinal artery, vein, and venules displays values in pseudo color.

#149760 - $15.00 USD Received 24 Jun 2011; revised 29 Jul 2011; accepted 29 Jul 2011; published 9 Aug 2011

Table 2. Vessel diameter, blood velocity, and flow in retinal venules; PO_2 and O_2 content in retinal venules and a major retinal artery in one rat

Blood Vessel	Diameter (μm)	Velocity (mm/s)	Flow (nl/min)	PO_2 (mmHg)	O_2 Content ($ml O_2$/dl)
Artery				35	8.1
Venule 1	16	4	51	22	3.5
Venule 2	11	4	21	23	3.7
Venule 3	16	4	44	27	5.2

Measured blood vessel diameter, velocity and calculated F in the draining venules connected to a major vein of one rat (shown in Fig. 2) are listed in Table 2. Measured PO_2 and O_2 content of blood in the major retinal artery and venules of the same rat are also listed in Table 2. PO_2 in the artery supplying the retinal area was assumed to be constant and the same as in the branching arterioles, since the branching arterioles are directly supplied by the major artery. It is not valid to use PO_2 in the major vein to calculate the local inner retinal MO_2 because the vein has substantial oxygen contributions from peripheral retinal tissue. Local inner retinal MO_2 was calculated according to Eq. (1) to be 4.5 nlO_2/min. The range of local inner retinal MO_2 measurements was from 3.6 to 11.4 nlO_2/min (5.1 ± 3.6 nlO_2/min; N = 5). Local inner retinal MO_2 measurements vary among rats depending on the volume of the retinal tissue drained by the selected venules.

4. Discussion

The feasibility of our methodology to measure quantitatively retinal blood flow and oxygen tension and to determine inner retinal metabolic rate of oxygen in rats was demonstrated. Our measurements in major retinal veins were in agreement with previously reported blood velocity [11,31] and vessel diameter [32] measurements in rats. Since blood velocity was determined by averaging velocities of multiple microspheres in each blood vessel, it is likely a reasonable estimate of the mean of the distribution of blood velocities that occur due to laminar flow. PO_2 measurements in retinal arteries and veins were consistent with values obtained with microelectrodes near the surface of retinal blood vessels in rats [33]. For comparison to previously published studies of retinal oxygen consumption, global inner retina MO_2 measurements obtained in the present study were divided by the estimated mass of inner retinal tissue in rat [34], yielding an average inner retinal oxygen consumption of 7.1 mlO_2/min*100g. This value is somewhat higher than inner retinal oxygen consumption measured by determining arteriovenous oxygen differences and blood flow in separate groups of pigs (4.6 and 3.8 mlO_2/min*100g) [35,36]. It is also higher than inner retinal oxygen consumption measurements obtained by oxygen microelectrodes for only a selected part of inner retina of rat, converted to the same units (1.1 mlO_2/min*100g) [5], and with retinal artery occlusion and 100% oxygen inspiration in cat and rat (3.7 and 2.7 mlO_2/min*100g) [7,8]. Differences in estimated parameters, such as the mass of inner retinal tissue, may in part account for variations of oxygen consumption values reported by various techniques.

In future studies, our method will allow investigation of the relationships among retinal blood flow, vascular oxygen levels, and oxygen consumption under normal and challenged physiological conditions. For example, by examining the same retinal tissue with and without light flicker, alterations in global and local inner retinal MO_2 measurements can be evaluated. Such studies will improve understanding of neurovascular coupling under a normal physiological condition, as well as assessment of abnormalities due to pathological states. Overall, quantitative measurements of inner retinal MO_2 have the potential to advance knowledge of retinal oxygen dynamics in health and disease.

#149760 - $15.00 USD Received 24 Jun 2011; revised 29 Jul 2011; accepted 29 Jul 2011; published 9 Aug 2011

Acknowledgments

The authors would like to acknowledge fruitful discussions with Dr. Charles Riva. NIH grants EY017918 and EY01792, senior scientific investigator award and an unrestricted departmental grant from Research to Prevent Blindness.

#149760 - $15.00 USD Received 24 Jun 2011; revised 29 Jul 2011; accepted 29 Jul 2011; published 9 Aug 2011